Density functional study of the interaction between small Au clusters, Au n (n = 1 – 7) and the rutile Ti O 2 surface. II. Adsorption on a partially reduced surface

Steeve Chrétien and Horia Metiu

Citation: The Journal of Chemical Physics **127**, 244708 (2007); doi: 10.1063/1.2806802
View online: http://dx.doi.org/10.1063/1.2806802
View Table of Contents: http://scitation.aip.org/content/aip/journal/jcp/127/24?ver=pdfcov
Published by the AIP Publishing

Density functional study of the interaction between small Au clusters, Au_n ($n=1-7$) and the rutile TiO_2 surface. II. Adsorption on a partially reduced surface

Steeve Chrétien[a] and Horia Metiu[b]
Department of Chemistry and Biochemistry, University of California, Santa Barbara, California 93106, USA

(Received 24 July 2007; accepted 16 October 2007; published online 28 December 2007)

We use density functional theory to examine the electronic structure of small Au_n ($n=1-7$) clusters, supported on a rutile $TiO_2(110)$ surface having oxygen vacancies on the surface (a partially reduced surface). Except for the monomer, the binding energy of all Au clusters to the partially reduced surface is larger by ~0.25 eV than the binding energy to a stoichiometric surface. The bonding site and the orientation of the cluster are controlled by the shape of the highest occupied molecular orbitals (HOMOs) of the free cluster (free cluster means a gas-phase cluster with the same geometry as the supported one). The bond is strong when the lobes of the HOMOs overlap with those of the high-energy states of the clean oxide surface (i.e., with no gold) that have lobes on the bridging and the in-plane oxygen atoms. In other words, the cluster takes a shape and a location that optimizes the contact of its HOMOs with the oxygen atoms. Fivefold coordinated Ti atoms located at a defect site ($5c$-Ti^*) participate in the binding only when a protruding lobe of the singly occupied molecular orbital (for odd n) or the lowest unoccupied molecular orbital (for even n) of the free Au_n cluster points toward a $5c$-Ti^* atom. The oxygen vacancy influences the binding energy of the clusters (except for Au_1) only when they are in direct contact with the defect. The desorption energy and the total charge on clusters that are close to, but do not overlap with, the vacancy differ little from the values they have when the cluster is adsorbed on a stoichiometric surface. The behavior of Au_1 is rather remarkable. The atom prefers to bind directly to the vacancy site with a binding energy of 1.81 eV. However, it also makes a strong bond (1.21 eV) with any $5c$-Ti atom even if that atom is far from the vacancy site. In contrast, the binding of a Au monomer to the $5c$-Ti atom of a surface without vacancies is weak (0.45 eV). The presence of the vacancy activates the $5c$-Ti atoms by populating states at the bottom of the conduction band. These states are delocalized and have lobes protruding out of the surface at the location of the $5c$-Ti atoms. It is the overlap of these lobes with the highest orbital of the Au atom that is the major reason for the bonding to the $5c$-Ti atom, no matter how far the latter is from the vacancy. The energy for breaking an adsorbed cluster into two adsorbed fragments is smaller than the kinetic energy of the mass-selected clusters deposited on the surface in experiments. However, this is not sufficient for breaking the cluster upon impact with the surface, since only a fraction of the available energy will go into the reaction coordinate for breakup. © *2007 American Institute of Physics*. [DOI: 10.1063/1.2806802]

I. INTRODUCTION

In this article we use density functional theory (DFT) to study the adsorption of Au_n ($n=1-7$) clusters on a partially reduced TiO_2 surface (partially reduced means that some oxygen atoms have been removed from the surface of the oxide). We are interested in the structure and the binding energy of the clusters, in the charge exchange between the cluster and the surface, in the energy needed to fragment the clusters, and in the interaction between coadsorbed clusters.

The interaction of Au with the reduced TiO_2 surface is of interest for several reasons. (1) Missing bridging oxygen atoms on the TiO_2 surface are believed to be nucleation centers for Au and Ag nanoparticles during vapor deposition experiments.[1–8] (2) It is believed that oxygen vacancies play an important role in catalysis. For example, Heiz and co–workers[9–11] have shown that Au_8 supported on a partially reduced MgO surface catalyzes CO oxidation at low temperature, while the same cluster deposited on the stoichiometric surface shows no reactivity. Yan *et al.*[12] showed that this is also true for clusters whose diameter exceeds 2 nm: CO conversion is proportional to the vacancy concentration prior to Au deposition on the surface. (3) Heiz and co-workers[9–11] performed density functional calculations which showed that the Au_8 cluster adsorbed on an oxygen vacancy becomes negatively charged and attributed the catalytic activity of the cluster to this charging effect. This is a reasonable assumption: gas-phase work has shown that Au clusters having an even number of electrons adsorb oxygen more weakly than the ones having an odd number of electrons.[13–27] In view of this, transferring electronic charge

[a]Electronic mail: steeve.chretien@videotron.ca.
[b]Electronic mail: metiu@chem.ucsb.edu.

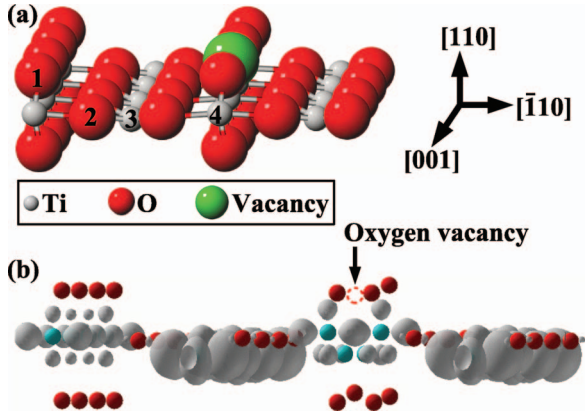

FIG. 1. (Color) (a) The top layer of a partially reduced rutile $TiO_2(110)$ surface. The atoms are labeled as follows: one bridging oxygen atom, two in-plane oxygen, three fivefold coordinated Ti atoms, four sixfold coordinated Ti atoms. (b) Density plot of one of the lowest energy eigenstates located at the minimum of the conduction band of a partially reduced surface. The plot shows an equal density surface of 0.02 $e/Å^3$.

to Au_8 is expected to make it more active. (4) TiO_2 is one of the most widely used supports for Au catalysis. (5) Recently it has become possible to deposit mass-selected clusters on oxide surfaces and study their properties.[2,10,11,28–44] The present work helps interpret the results of such experiments.

To give a brief preview of our main results, we need to define the structural features of the partially reduced rutile $TiO_2(110)$ surface (see Fig. 1). The surface layer contains bridging oxygen atoms (labeled 1 in the figure), in-plane oxygen atoms (labeled 2 in the figure), and fivefold coordinated Ti atoms (denoted 5*c*-Ti and labeled 3 in the figure). The remaining Ti atoms are sixfold coordinated (denoted 6*c*-Ti, and labeled four in the figure). By far the most common oxygen vacancy on the surface is a missing bridging oxygen[45] shown in Fig. 1 as a green sphere in the bridging oxygen atom row. Upon removal of a bridging oxygen atom, two 6*c*-Ti atoms become fivefold coordinated and we denote them 5*c*-Ti*.

The density functional calculations reported here show that the creation of oxygen vacancies populates the bottom of the rutile $TiO_2(110)$ conduction band with electrons. The adsorption of the cluster creates a molecular orbital that consists of an empty orbital of the cluster and the orbital located in the conduction band of the oxide. Charge is transferred to the Au cluster when this molecular orbital is located below the conduction band.

The presence of a vacancy increases the binding energy of the Au clusters by at most 0.32 eV (compared to the bond the same cluster makes with the stoichiometric surface). Au_1 is an exception and its binding energy is 1.36 eV higher than the binding on the stoichiometric surface. Electron transfer from the 5*c*-Ti atoms located at the vacancy site to the Au_n clusters plays a minor role in the cluster binding. Only Au_1 and Au_3 gain electronic density (becoming negatively charged) in their lowest energy structure. Au_2, Au_4, and Au_6 stay neutral, while Au_5 and Au_7 transfer electrons to the reduced surface becoming positively charged, even though they are adsorbed at the location of a missing oxygen atom.

We find that the bonding geometry is controlled by the shape of the highest occupied orbitals of the free cluster (by free cluster we mean a cluster obtained by freezing the geometry of the adsorbed cluster and removing the oxide) and the high-energy orbitals of the clean surface (the surface with no cluster on it).

The main contribution to the binding is the overlap between the highest occupied molecular orbitals (HOMOs) of Au_n and eigenstates of the clean, reduced oxide localized on the bridging and the in-plane oxygen atoms. The same binding mechanism was observed for Au clusters binding to the stoichiometric surface.[46] This explains the fact that Au_n clusters ($n=2$, 5–7) prefer to interact with bridging oxygen atoms located on each side of the defect rather than to the 5*c*-Ti* atoms located at the defect site. The absence of a bridging oxygen atom allows the cluster to maximize the orbital overlap with the oxygen atoms bordering the vacancy, in the bridging oxygen row.

Fivefold coordinated Ti atoms located in the surface layer or at the vacancy site play a secondary role in the Au_n cluster binding to the partially reduced surface. We find that 5*c*-Ti atoms participate in the cluster binding in only two cases: (1) the singly occupied molecular orbital (SOMO) for odd n or the lowest unoccupied molecular orbital (LUMO) for even n points toward the 5*c*-Ti* atoms or (2) the SOMO points toward a 5*c*-Ti atom. This results in the formation of a MO involving the 5*c*-Ti atoms and the Au cluster, which becomes partially filled through an electron transfer from the oxide conduction band. Therefore, Au_n clusters become negatively charged when 5*c*-Ti atoms participate in the binding. The importance of the shape and the orientation of the LUMO for even n (and SOMO for odd n) is nicely illustrated by considering different ligations of the same gas-phase cluster to a vacancy site (i.e., adsorbed clusters having the same number of atoms but differing through their location or their orientation with respect to the vacancy and/or the surface). For example, Au_2 in its lowest energy structure does not exchange charge with the surface on the partially reduced surface, indicating that 5*c*-Ti atoms do not participate in the dimer binding. On the other hand, for the second-lowest energy isomer of Au_2 5*c*-Ti atoms participate significantly in binding resulting in a charge accumulation of 0.7e on the dimer.

The effect of the vacancy is fairly local: the binding energy of a cluster next to the vacancy (but not overlapping with it) is close to the binding energy to the stoichiometric surface. The absence of a long range attraction force between the defect and a cluster adsorbed next to it can be explained by the binding mechanism presented above. On a stoichiometric region of a partially reduced surface, the cluster changes its shape and orientation in order to maximize the orbital overlap between its frontier MOs and the eigenstates of the clean oxide involving bridging and in-plane oxygen atoms. As a consequence, the LUMO for even n and the SOMO for odd n do not point in the direction of a 5*c*-Ti atom. This prevents the formation of a binding MO involving 5*c*-Ti atoms and, consequently, no charge can be exchanged between the cluster and the partially reduced support.

The behavior of Au_1 differs from that of the larger clusters because its SOMO points toward a 5*c*-Ti atom every

time the monomer is in contact with a 5*c*-Ti atom. This allows the formation of a partially filled, bonding MO involving the monomer SOMO and the eigenstates of the clean, reduced oxide localized on 5*c*-Ti atoms. This MO is located in the band gap of reduced, rutile TiO_2(110). The monomer adsorption energy increases (relative to the value obtained for the stoichiometric surface) every time an electron transfer populates this bonding state. This is why the binding energy of a monomer to a vacancy site is 1.36 eV larger than the adsorption energy on the stoichiometric surface. Moreover, the monomer binding energy to any 5*c*-Ti atom is ~1.20 eV, regardless of how far it is from the vacancy site, because the states of the clean oxide involved in the formation of a binding MO with the monomer have lobes on all the 5*c*-Ti atoms of the surface layer.

II. COMPUTATIONAL DETAILS

DFT calculations have been performed with the VASP program[47–50] with the functional of Perdew and Wang 1991 (PW91) (Refs. 51–54) and scalar relativistic ultrasoft pseudopotentials.[55] We used a soft or a hard pseudopotential for describing the oxygen atoms. The cutoffs in the plane-wave expansion were 270 eV, in calculations involving the soft-oxygen pseudopotential, and 396 eV in the other case. The energy differences between the results obtained with the two pseudopotentials are less than 0.1 eV. This difference is smaller than the expected accuracy of DFT.

Due to the large supercell we sample the Brillouin zone at the Γ point only. Comparison with calculations performed by Pillay and Hwang[56] on the same systems using a smaller supercell and a $(2\times4\times1)$ Monkhorst-Pack mesh allows us to believe that our desorption energies are converged within 0.1 eV. Monopole, dipole, and quadrupole corrections to the energy were taken into account using a modified version of the method proposed by Makov and Payne.[57] A Harris-Foulkes-type correction to the forces was included. The Kohn-Sham matrix was diagonalized iteratively using the residual minimization method-direct inversion in the iterative subspace.[50,58] Fractional occupancies of the bands were allowed using a window of 0.05 eV and a Gaussian smearing.

Many starting structures (more than 30 for all clusters larger than the dimer) corresponding to the adsorption of Au_n on the partially reduced surface have been fully optimized, without symmetry constraints, by using a conjugated-gradient algorithm.[59] Various configurations for a given gold cluster were considered, including three-dimensional and metastable structures located up to 2 eV above the ground state, based on calculations performed for the unsupported (gas-phase) neutral, cationic, and anionic Au clusters, Au_n^q $(n=1-7,\ q=-1,\ 0,\ +1)$. The lowest energy structures of the gas-phase clusters agree with the ones previously reported in the literature.[60–66] A 12 layer (four triple layers) slab has been used. All atoms in the solid and the clusters were relaxed except for the bottom triple layer of the TiO_2(110) slab which were fixed to the bulk positions. The adsorption of Au clusters takes place on only one side of the TiO_2(110) slab. The vacuum space above the slab was 17 Å thick. The convergence criterion was 10^{-4} eV for the self-consistent electronic minimization and for the change of the total free energy between two consecutive ionic steps.

The difference N_s between the number of electrons with spin up and down was fixed during the geometry optimization. We have performed spin-restricted calculations for the systems containing an even number of electrons (N_s was fixed to 0) and spin polarized when the number of electrons was odd (N_s was fixed to 1). At convergence, all the optimized structures having a gap smaller than 0.5 eV between the highest occupied and lowest empty eigenstates were optimized again using spin-polarized formalism and the number of unpaired electrons initially used was increased by 2. For each stable structure we report the lowest energy produced in such calculations.

The atomic charges were obtained from Bader's analysis[67] based on the numerical implementation developed by Henkelman *et al.*[68,69] The change of the electron charge on the cluster is obtained by calculating the charge on the gold atoms of the adsorbed cluster and then subtracting the total charge of the gas-phase cluster. A negative number indicates that the Au cluster gains electronic charge when it is adsorbed.

In this paper, the terms two dimensional (2D) and three dimensional (3D) refer to the definition use to characterized bare clusters in the gas phase. On the other hand, the terms one-, two-, and three-layer high clusters indicate the thickness of the adsorbed Au clusters, in the direction normal to the surface. Therefore, a planar cluster (2D) adsorbed perpendicularly to the surface can be a two-layer high cluster [e.g., see the structure shown in Figs. 2(d) and 2(l)] or a three-layer high cluster [e.g., see the structure shown in Figs. 2(f) and 2(m)] depending on how it binds to the surface.

We use the term desorption energy (D_e) to describe the binding of the Au clusters to the surface and the term dissociation energy (δ_e) to indicate the energy required to fragment a cluster into two pieces.

The desorption energies are obtained using

$$D_e[\mathrm{Au}_n] = E[\mathrm{TiO}_2] + E[\mathrm{Au}_n] - E[\mathrm{Au}_n/\mathrm{TiO}_2]. \quad (1)$$

Here, $E[\mathrm{TiO}_2]$ and $E[\mathrm{Au}_n/\mathrm{TiO}_2]$ are the total energies of a partially reduced rutile TiO_2(110) surface without and with a Au cluster on its surface, while $E[\mathrm{Au}_n]$ is the total energy of Au_n at its equilibrium structure in the gas phase.

The dissociation energy δ_e of a supported Au clusters is calculated using

$$\delta_e[\mathrm{Au}_n] = E[(\mathrm{Au}_x + \mathrm{Au}_{n-x})/\mathrm{TiO}_2] - E[\mathrm{Au}_n/\mathrm{TiO}_2]. \quad (2)$$

Here, $E[\mathrm{Au}_n/\mathrm{TiO}_2]$ is the total energy of the lowest energy structure of the intact cluster adsorbed on a partially reduced TiO_2(110) surface. $E[(\mathrm{Au}_x+\mathrm{Au}_{n-x})/\mathrm{TiO}_2]$ is the total energy of the fragmented clusters simultaneously present on the surface inside the surface unit cell; one fragment is adsorbed at its equilibrium location at the vacancy site; the other is adsorbed on the stoichiometric area of the surface. The fragments are separated by at least 6 Å from each other and from their periodic replicas. After placing the fragments at the locations mentioned above, the geometry off all atoms is

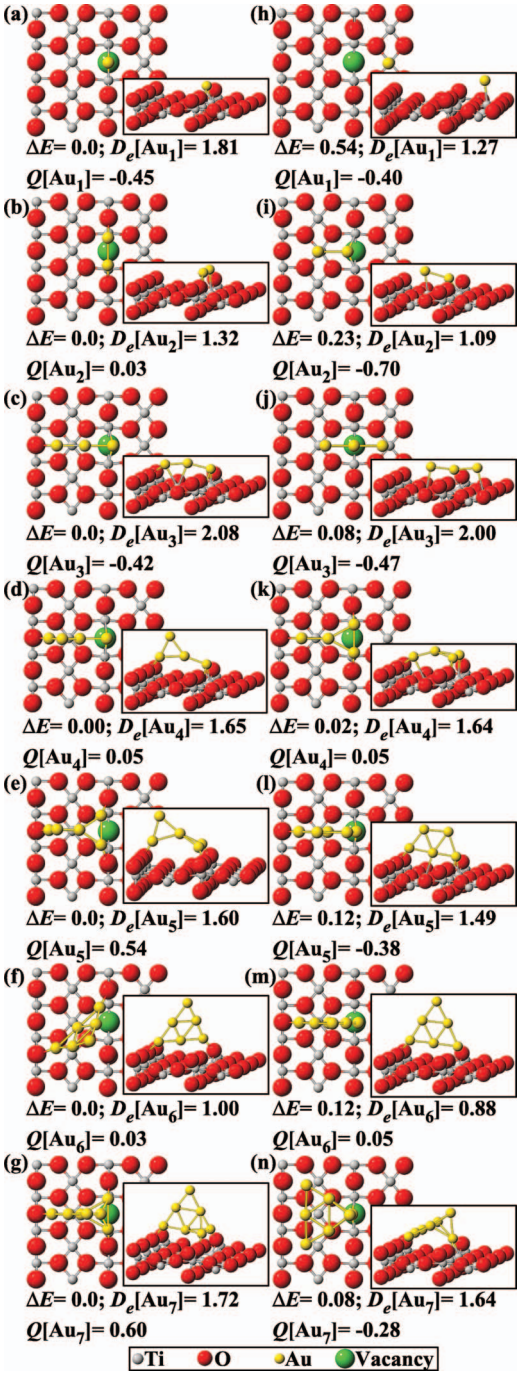

FIG. 2. (Color) Relative (ΔE) and desorption (D_e) energies of the two lowest energy structures corresponding to the adsorption of Au clusters, Au_n ($n=1-7$) on a partially reduced rutile $TiO_2(110)$ surface. [(a)–(g)] Equilibrium structure. [(h)–(n)] Second-lowest energy isomer. The energies are in eV and were obtained with the PW91 functional and the hard-oxygen pseudopotential using a $[4\times2]$ supercell and 12 layer slab.The change of the electronic charge on the Au clusters upon adsorption, Q, was obtained from Bader's charge analysis (Ref. 68).

optimized. The dissociation is an endothermic process when δ_e is positive.

It has been long suspected that the properties of oxides having narrow d bands, such as rutile TiO_2, might not describe correctly because of the electron self-interaction inherent in the DFT functionals based on the generalized gradient approximation (GGA). It is not clear yet which properties of which oxides are affected by the shortcomings of GGA, nor do we have a measure of the magnitude of the errors. An excellent review of the situation, for oxygen vacancy formation on oxide surfaces, has been published recently by Ganduglia-Pirovano *et al.*[70] The formation of oxygen vacancies on the rutile $TiO_2(110)$ surface was recently studied by Di Valenti, *et al.*[71] They assumed, reasonably, that the results obtained by using hybrid functionals, which remove some of the self-interaction, are closer to the truth than those obtained with GGA-DFT. They found that using the B3LYP functional[72,73] the electrons left behind, when an oxygen vacancy is formed, are in an orbital localized around the two Ti atoms to which the oxygen atom was bound (formally turning two Ti^{+4} ions into two Ti^{3+}). In the GGA calculations the electrons are more delocalized. In GGA the reduced oxide is conducting, while in B3LYP the electrons left behind are in an orbital located in the band gap. The B3LYP results are consistent with the experimental observations,[45] while the GGA ones are not. It is not clear to what extent these discrepancies between the properties of the orbitals in GGA and B3LYP affect the results presented here, especially the binding energies.

Orbital properties should be used cautiously. The purpose of the Kohn-Sham equation is to generate the correct electron density and the Kohn-Sham orbitals and their energies are not physical observables. Nevertheless, their use for rationalizing chemical behavior has been very successful, even though it lacks a rigorous basis. We regard the orbital-based interpretations, of the kind used here, to be a means for rationalizing the energies and the structures *produced by the GGA-DFT calculations*; if these energies and structures are correct, the rationalization helps us understand reality. Among the explanations provided here, those based on the existence of delocalized electrons in the conduction band of the reduced oxide are most likely to change when B3LYP calculations are used. The description of the cluster structure and of the charge transfer within B3LYP theory may be different than the one offered for GGA-DFT.

III. THE PARTIALLY REDUCED RUTILE $TiO_2(110)$ SURFACE

We have already explained the structural features of the partially reduced, rutile $TiO_2(110)$ surface in the Introduction. The partially reduced surface is obtained by removing one of the protruding oxygen atoms. For the $[4\times2]$ and $[5\times2]$ supercells used here, this corresponds to a bridging-oxygen vacancy concentrations of 12.5% and 10%, respectively.

The energy required to remove one bridging oxygen atom from the stoichiometric rutile $TiO_2(110)$ surface to form a partially reduced surface and half an oxygen molecule in the gas phase is called the vacancy formation energy (E_{vf}). It is computed using

$$E_{vf} = E[TiO_2(r)] + \tfrac{1}{2}E[O_2] - E[TiO_2(s)]. \quad (3)$$

Here, $E[TiO_2(r)]$ and $E[TiO_2(s)]$ are, respectively, the energies of the partially reduced and stoichiometric rutile $TiO_2(110)$ surfaces, while is $E[O_2]$ the energy of O_2 in the gas phase. Within the current computational setup, E_{vf} is

3.6 eV. This is in good agreement with the value of 3.5 eV reported in the literature for similar oxygen vacancy concentration and supercell dimension.[74]

Our calculations show that when rutile TiO_2(110) is reduced, electrons fill states at the bottom of the conduction band. These states play an important role in explaining some of the results of the present computations. A typical eigenstate of this kind is shown in Fig. 1(b). It is important to note, for what follows, that the electron density in these states is spread over all the 5*c*-Ti atoms, not only over those located near the defect site.

IV. THE BINDING MECHANISM OF Au_n TO THE PARTIALLY REDUCED RUTILE TiO_2(110)

A. The binding energies and the geometries of the adsorbed Au_n clusters having the lowest energy

The structures of the Au_n clusters ($n=1-7$) adsorbed on a partially reduced rutile TiO_2(110) surface are shown in Fig. 2. The lowest energy structures are in the left-hand side and the structures having the second-lowest energy in the right-hand side. We have found many other structures corresponding to minima on the potential energy surface, which have higher energy than the ones shown in Fig. 2. All the structures whose energy is less than 0.3 eV above that of the lowest energy structure were included in the present analysis.

The results for the binding energy, the binding site, and the geometry of the smallest clusters ($n=1-4$) agree with those published previously.[3,56,75] For clusters larger than tetramers we found geometries and binding sites having lower energies than those published by Wang and Hammer[76] and Matthey *et al.*[77] We suspect that the low-energy structures we have found were not studied in previous work.

Given the general (and reasonable) belief that a vacancy site is very reactive, one would expect that all clusters prefer to bind, whenever possible, by placing one Au atom at the site from which the oxygen has been removed. This is indeed the case for Au_1, for which the desorption energy from a vacant site is 1.81 eV [Fig. 2(a)], while it is 1.27 eV when it binds to a 5*c*-Ti atom located next to a vacancy site [Fig. 2(h)]. Both isomers of Au_3 place a Au atom in the vacancy site. For Au_4, the isomer with a Au atom in the vacancy [see Fig. 2(d)] has the same energy as the isomer for which Au_4 binds to two bridging-oxygen atoms located on each side of the vacancy site [see Fig. 2(k)]. All other stable isomers prefer a ligation in which the cluster binds to the two oxygen atoms adjacent to the vacancy. Clearly, there is no universal propensity for placing a Au atom in the vacant site.

In gas phase all clusters examined here are planar and one would think, perhaps naively, that they will bind parallel to the surface so that the Au atoms will have the highest contact with the surface atoms. This is not the case for the larger clusters: the clusters bind more strongly by making two-layer high or three-layer high structures so that the edge atoms point toward the bridging-oxygen atoms [e.g., Figs. 2(d)–2(g) and 2(l)–2(n). We will explain the reason for this tendency in Sec. IV D.

The binding energy of the Au clusters to the reduced surface exceeds the binding energy to the stoichiometric surface by at most 0.32 eV (see Table I). The only exception is Au_1 whose binding energy exceeds that on the stoichiometric surface[46] by 1.36 eV. As we show below Au_1 is peculiar in other respects, and our model of the bonding must explain its behavior. The increase in the binding energy of gold clusters by the reduction of TiO_2 is much smaller than that observed for the gold clusters binding to MgO. For example, Au_8 binds more strongly to the reduced MgO(100) surface than to the stoichiometric surface by ~2.2 eV.[9,11] This is probably due to the fact that MgO is much harder to reduce than TiO_2, which suggests that defects (missing oxygen atoms) on MgO are more reactive. Part of the reason for this difference is the ability of Ti to make tetravalent and trivalent oxides, which makes the removal of an oxygen atom less traumatic than in the case of Mg, which lacks this adaptability.

TABLE I. Desorption energy (D_e) of Au_n clusters ($n=1-7$) from a stoichiometric and a partially reduced rutile TiO_2(110) surfaces. D_e are in eV and were obtained with the combination of the PW91 functional and the hard-oxygen pseudopotential using a $[4\times2]$ supercell and a 12 layer thick slab.

		Reduced	
n	Stoichiometric	Equilibrium[a]	Charging[b]
1	0.45	1.81	1.81
2	1.06	1.32	1.09
3	1.76	2.08	2.08
4	1.37	1.65	1.40
5	1.49	1.60	1.49
6	0.78	1.00	0.49
7	1.56	1.72	1.64

[a]Desorption energies computed for the equilibrium structure.
[b]Desorption energies of the lowest energy structure in which an electron transferred from the vacancy site to the Au clusters is taking place. For example, for Au_2 this is the energy of the isomer shown in Fig. 2(i) which is the lowest energy Au_2 cluster that is negatively charged.

B. The effect of the vacancy on the cluster-surface bond is localized

To find to what extent the binding energy of the Au clusters depends on the distance between their binding site and the vacancy, we have performed the calculations summarized in Fig. 3. For example, for Au_4 we have examined four isomers that differ through either the shape of the cluster or its location on the surface, or both [see Figs. 3(c), 3(d), and 3(f)]. All the structures shown in Figs. 3(c)–3(f) correspond to minima on the potential energy surface. In Fig. 3 we give the binding energy of the cluster to the reduced surface and, in brackets, the binding energy to the stoichiometric surface[46] (at the same site and for a cluster of the same shape). We also give the charge on the cluster when it is bound to the reduced or the stoichiometric surface (the latter is in brackets). It is clear that as long as the cluster does not make contact with the vacancy, its binding energy and its charge on a reduced surface are very close to the values obtained for the stoichiometric surface. The only exception is Au_1 whose binding energy is dramatically increased by the presence of a vacancy. Au_1 binds strongly to 5*c*-Ti atoms even if they are rather far from the location of the vacancy.

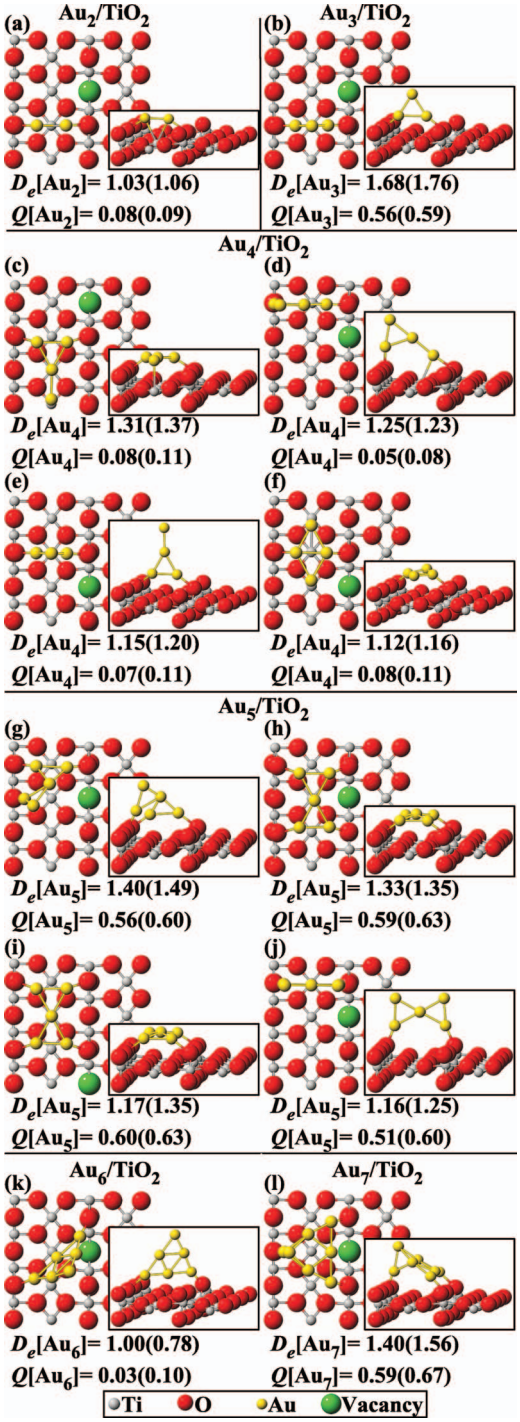

FIG. 3. (Color) Desorption energies (D_e) of some structures corresponding to the adsorption of Au_n clusters (n=2–7) next to a missing bridging oxygen (defect) atom on a reduced rutile TiO_2(110) surface. Q is the total electronic charge on the Au clusters obtained from Bader's analysis (Ref. 68). In parenthesis we indicate the values obtained on a stoichiometric surface for the same ligation (geometry). The energies are in eV and were computed with the PW91 functional and the hard-oxygen pseudopotential on a [4×2] supercell and a 12 layer slab.

C. The charge exchange between the adsorbed Au_n (n=2–7) and the reduced TiO_2

The removal of a bridging-oxygen atom, to create an oxygen vacancy, leaves behind two electrons that used to be tied up in the Ti–O bonds; one could think qualitatively of the vacancy as a "radical," a site that is ready to donate electrons to a molecule located there. It is for this reason that it is widely believed (see, for example, Ref. 56) that the Au clusters, which have high electron affinities,[78,79] will become negatively charged when they bind at the vacancy site.

Our calculations show that this is not always the case. Among the lowest energy structures only Au_1 and Au_3 are charged negatively upon chemisorption, Au_2, Au_4, and Au_6 exchange practically no charge with the substrate, and Au_5 and Au_7 are charged positively [see Figs. 2(e) and 2(g), respectively]. Note that Au_3 and Au_4 are the only low-energy clusters that place an atom in the vacancy but this does not control charge transfer: Au_3 is negatively charged but Au_4 exchanges no charge. Therefore, direct contact with the vacancy site is not sufficient for electron transfer from the surface to the cluster.

The electronegativity (or the electron affinity) of the cluster in gas phase is also a poor indicator of a cluster's ability to extract charge from the surface. For example, the lowest energy Au_2 exchanges no charge [Fig. 2(b)], while the next-lowest energy Au_2 cluster has a charge of $-0.7e$ [Fig. 2(i)]. They both originate from the same gas-phase cluster and differ only through their position on the surface. If the propensity to exchange charge would be controlled by the electron affinity alone, the two clusters would draw the same amount of charge. A similar observation can be made about Au_7. The lowest energy adsorbed cluster is positively charged ($+0.60e$) [see Fig. 2(g)], while the second-lowest energy one is negatively charged ($-0.28e$) [see Fig. 2(n)]; the shape of the cluster is the same in both cases, but their position with respect to the vacancy is not. These observations do not depend on the choice of a particular pseudopotential. We have repeated the calculations of the lowest two energy isomers, corresponding to Au_7 adsorption on a partially reduced TiO_2(110) surface, using the projector augmented wave (PAW) pseudopotential.[80,81] Au_7 loses $0.57e$ in the most stable isomer [Fig. 2(g)], while it gains $0.25e$ in the second-lowest energy isomer [Fig. 2(n)].

A final argument that taking electrons from the substrate does not control the binding strength of the cluster to the oxide is presented in Table I. This compares the desorption energy of a cluster from the stoichiometric surface (column 2) to the desorption energy from the partially reduced surface (column 3). In the fourth column we show the desorption energy for the lowest energy isomer that gains electron charge from the support when it binds. For example, for Au_2 the second-lowest energy isomer is the lowest energy isomer that gains charge from the substrate and its desorption energy is 1.09 eV [see Fig. 2(i)]. For Au_4, neither the lowest energy isomer nor the second-lowest energy one gains charge when they bind to the substrate, and we have listed in Table I (in the fourth column) the desorption energy of the fifth-lowest isomer (1.40 eV) which is the first one to gain charge [this isomer is shown in Fig. 4(c) of Ref. 82]. The values reported for the monomer and the trimer are the same in the third and fourth columns because these are the only two cases where charging is observed in the lowest energy isomer (see Fig. 2). We see a systematic trend. The desorption energy from the partially reduced surface is closer to the desorption energy from the stoichiometric surface when a cluster is able to take

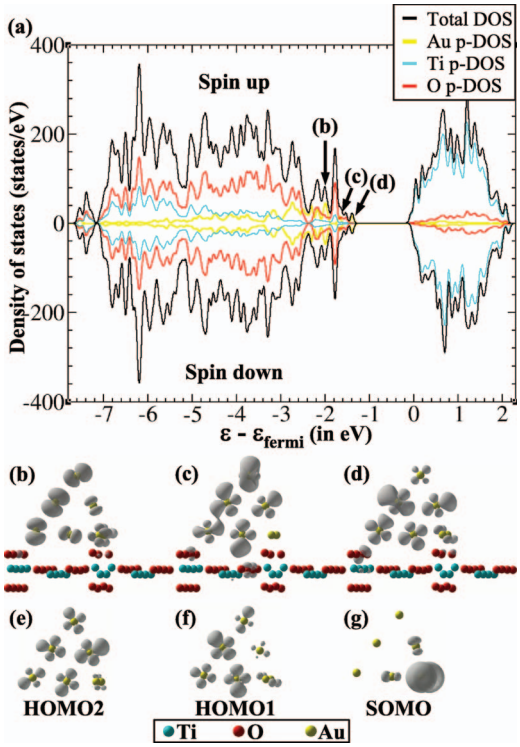

FIG. 4. (Color) (a) Total and atom-projected density of states (DOS) around the Fermi level corresponding to Au_7 adsorbed on a partially reduced rutile $TiO_2(110)$ surface [see structure display in Fig. 2(g)]. [(b)–(d)] Density plots of the highest occupied eigenstates localized on Au_7 when supported on a partially reduced $TiO_2(110)$. [(e)–(g)] Density plots of the frontier molecular orbitals of Au_7 in the gas phase having the same structure and orientation as in Fig. 2(g). Density plots show equal density surfaces of 0.02 $e/Å^3$.

electrons from the substrate. Surprisingly, the Au_6 desorption energy from the lowest energy structure in which Au_6 is gaining electrons is smaller by 0.29 eV than the one observed on the stoichiometric surface. Thus, the larger desorption energies observed on the partially reduced surface compared to the stoichiometric one are not due to charge transfer from the vacancy site into the cluster.

We will show in the next subsection that these observations are best explained by the shape of the frontier orbitals of the free clusters.

D. Orbital overlap and the bonding between Au_n and reduced TiO_2

In a crude approximation, the bond energy and the charge transfer between the cluster and the surface are most affected by the formation of the frontier orbitals of the Au_n/TiO_2 system, in which the electron has a high probability of being localized on the adsorbed Au clusters. Such orbitals can be thought off as linear combination between the frontier molecular orbitals of two entities. One is a gas-phase cluster having the same shape as the adsorbed cluster (we call this a free cluster). The other is the surface in the absence of the cluster (we call this the "clean" surface). Such a combined orbital will have lobes localized on the adsorbed cluster but will also extend over a region of the oxide. A necessary condition for the formation of such orbitals is the overlap between the frontier orbitals of the free cluster and a frontier orbital of the clean surface. Therefore, the position of the cluster on the surface and its orientation will be controlled by the need to create a good overlap of these orbitals. In what follows we test this hypothesis and identify the orbitals that most affect bond formation and charge exchange. We stress that interpretations based on such arguments are qualitative and are justified mainly by their agreement with the results of the DFT calculations.

To illustrate how this idea works we examine the Au_7 isomers shown in Figs. 2(g) and 2(n). In these isomers the Au_7 cluster has practically the same structure; they differ only through the location with respect to the vacancy and the orientation with respect to the surface.

To understand the nature of the bond in the lowest energy isomer of Au_7 [Fig. 2(g)], we have plotted in Fig. 4 the total density of states (DOS) and the site-projected DOS for Au, Ti, and O. In this plot, the rutile $TiO_2(110)$ valence band is on the left and the conduction band on the right. In the site-projected DOS, the wave function character is obtained by projecting each eigenstate onto spherical harmonics that are nonzero within a sphere of radius R centered on each atomic site. Radii of 1.503, 1.323, and 0.741 Å have been used, respectively, for Au, Ti, and O.

The frontier molecular orbitals of Au_7/TiO_2 that are localized on Au_7 (yellow line) contain contributions from the valence band of the clean oxide, which has mostly O $2p$ character (red line), and a small contribution from the Ti atoms (cyan line). Density plots ($|\varphi_i|^2$) of the three highest occupied eigenstates φ_i of Au_7/TiO_2, which are localized on Au_7, are provided in Figs. 4(b)–4(d) (the orbital energy increases from left to right). Density plots of frontier molecular orbitals of the free Au_7 are presented in Figs. 4(e)–4(g). The same conclusions would have been reached, had we used the orbitals of the optimized gas-phase structure of the neutral clusters having the same shape as the supported ones. The energy of these orbitals grows in the order HOMO2, HOMO1, and SOMO. The density plots in Figs. 4(b)–4(d) show that the high-energy molecular orbitals of the Au_7/TiO_2 are combinations of the HOMOs of free Au_7 cluster and the eigenstates of the clean oxide localized on the bridging oxygens and on the in-plane oxygens. For example, one can see that HOMO2 and HOMO1 of Au_7 are involved in the states displayed in Figs. 4(d) and 4(c), respectively. Such combinations can be formed only if the adsorbed cluster takes a position in which the lobes of its HOMOs point toward the bridging oxygen and/or the in-plane oxygen atoms on the surface of the oxide. Thus we reach our first qualitative conclusion: the location and the orientation of the lowest energy Au_7 cluster are controlled mainly by the overlap of the lobes of its HOMO orbitals with the bridging and the in-plane oxygen atoms.

The SOMO of the free Au cluster does not participate in the formation of a filled molecular orbital of the Au_7/TiO_2 system. Its lobes are directed toward the bridging oxygen atoms located on each side of the vacant site to form an orbital of the Au-oxide system whose energy is above the bottom of the conduction band. When this orbital is formed, the electron that was in the SOMO of Au_7, prior to the cluster-oxide bond formation, will flow into the conduction

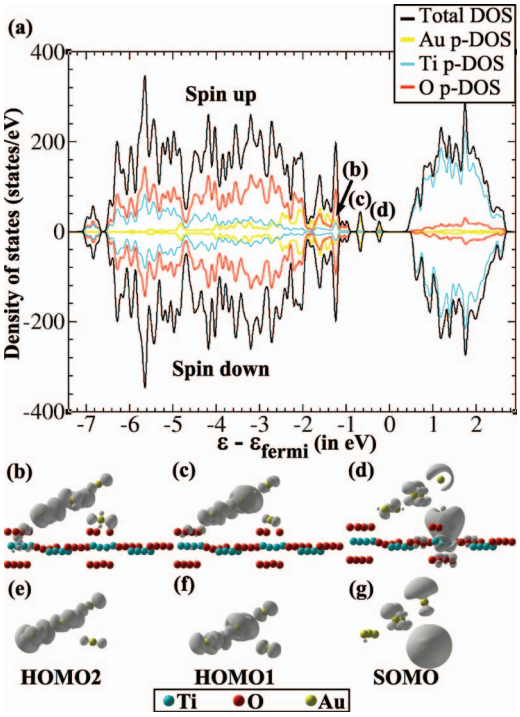

FIG. 5. (Color) Same as Fig. 4 but for structure display in Fig. 2(n).

band. This charge transfer results in an accumulation of a positive charge on Au_7, which explains qualitatively the Bader's charge provided in Fig. 2.

The second-lowest energy isomer of Au_7 [see Fig. 2(n)] behaves differently from the lowest energy one. In particular, it is charged negatively and one of its atoms points into the vacant site. To understand its behavior we need to remember that the presence of oxygen vacancies on the surface places electrons at the bottom of the conduction band. The orientation of the cluster on the surface [see Fig. 2(n)] is such that a lobe of the SOMO of the free cluster protrudes in the direction of the $5c$-Ti* atoms [see Fig. 5(g)]. This allows the formation of a bonding state between the SOMO of the free cluster and the eigenstates of the clean oxide located in the conduction band of $TiO_2(110)$ and localized on $5c$-Ti* atoms [see Fig. 5(d)]. The energy of this bonding state is in the band gap, as shown by the projected DOS provided in Fig. 5(a). This allows electronic charge to flow into this state from the conduction band, charging the cluster negatively [see Fig. 2(n)]. This is in agreement with the negative Bader charge calculated by DFT [see Fig. 2(n)].

In comparing the results for the two isomers of Au_7, we see that the shape and the orientation of the SOMO of Au_7 with respect to the surface explain how the presence of the vacancy modulates the charge exchange between the cluster and the surface (see Fig. 3). If a large lobe of SOMO points directly to the $5c$-Ti*, the cluster is negatively charged; if it points to the oxygen atoms (bridging or in plane), the cluster will be charged positively.

Forming a combination with orbitals localized on the $5c$-Ti* atom is not the only way a $5c$-Ti atom can affect the properties of the adsorbed cluster. A bonding state between Au_n and $5c$-Ti is observed in the band gap every time a lobe of SOMO points toward a $5c$-Ti atom located in the surface

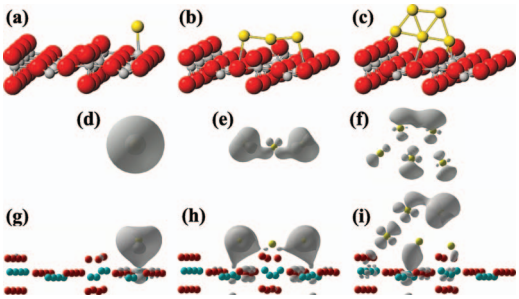

FIG. 6. (Color) [(a)–(c)] Second-lowest energy isomer corresponding to the adsorption of Au_1, Au_3, and Au_5 on a partially reduced rutile $TiO_2(110)$. [(d)–(f)] Density plots of the SOMO of Au_1, Au_3, and Au_5 in the gas phase having the same orientation as in the structure (a)–(c). [(g)–(i)] Density plots of the HOMO localized on Au_1, Au_3, and Au_5 for structures (a)–(c). We used the PW91 functional with a $[4\times2]$ supercell and a 12 layer slab. Density plots show equal density surface of 0.02 $e/Å^3$.

layer. This happens because the eigenstates located at the bottom of the conduction band possess amplitude over all the $5c$-Ti atoms located in the top layer [see Fig. 1(b)]. This is illustrated by the second-lowest energy structures of Au_1, Au_3, and Au_5. The orientation of these adsorbed clusters with respect to the surface is such that the lobes of their SOMOs point toward the $5c$-Ti atoms on the surface. When the free cluster is brought in contact with the clean oxide, a bonding state is formed by combining the SOMO with a state of the oxide that is located in the conduction band and has lobes on the $5c$-Ti atoms on the surface [see Figs. 6(g)–6(i)]. These states are located in the band gap allowing electronic density to flow from the conduction band into the cluster. This explains the negative Bader charges in Figs. 2(b), 2(j), and 2(l).

Au_n clusters with even n do not have a SOMO. In these clusters, the LUMO plays the same role as the SOMO does for odd n. The LUMO of the free cluster participates in the formation of a bonding molecular orbital in the Au_n/TiO_2 system only when the orientation of the free cluster is such that a lobe of its LUMO points in the direction of the $5c$-Ti* atoms. This is shown for Au_2/TiO_2 in Fig. 7. The LUMO of the free dimer [see Fig. 7(d)] does not participate in the formation of a filled molecular orbital in the lowest energy structure of Au_2/TiO_2 [see Fig. 7(a)] because the orientation of the dimer is such that its LUMO protrudes in the direction of the bridging oxygen atoms located on each side of the defect site [see Fig. 7(e)]. As for Au clusters with odd n, the resulting molecular orbital is above the conduction band of the oxide. In contrast to Au clusters with odd n, the clusters having even n stay neutral when this situation exists because LUMO is empty while the SOMO is partially filled. The orientation of the dimer in the second-lowest energy isomer allows the formation of a bonding orbital involving the $5c$-Ti* atoms because a lobe of its LUMO is pointing in the direction of the vacancy site, as shown in Fig. 7(f). The resulting molecular orbital is located in the band gap allowing electronic density to flow in from the conduction band. This explains the charge accumulation observed in the second-lowest energy isomer [see Fig. 2(i)]

In summary, the state formed by the overlap of the SOMO (or LUMO for even n) and the eigenstates located in the conduction band of rutile $TiO_2(110)$ is below the bottom

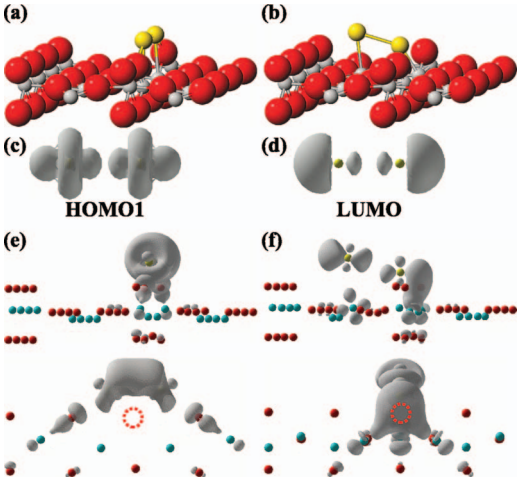

FIG. 7. (Color) [(a)–(b)] Lowest energy isomers corresponding to Au_2 adsorption on a partially reduced rutile TiO_2(110). (c) Density plots of the HOMO of Au_2 in the gas phase. (d) Density plots of the LUMO of Au_2 in the gas phase. [(e)–(f)] Density plots of the HOMO localized on Au_2 for structures (a) and (b). Two views are shown: the one on the top is the same as the one display in (a) and (b), while the one at the bottom show density plots along the $[1\bar{1}0]$ direction (see Fig. 1 for definition). The vacancy site is indicated by a red dotted circle. We used the PW91 functional with a $[4\times2]$ supercell and a 12 layer slab. Density plots show equal density surface of 0.02 $e/Å^3$.

of the conduction band when the SOMO (or LUMO for even n) points in the direction of a 5c-Ti, resulting in an accumulation of a negative charge on the cluster. When the SOMO (or LUMO for even n) points toward the bridging oxygen or the in-plane oxygen atoms, the energy of the molecular orbital involving the SOMO (or LUMO for even n) is above the bottom of the conduction band. Some electron density is lost by odd clusters because their SOMO is partially filled prior to the formation of the bonding molecular orbital, while the even clusters stay neutral because their LUMO is empty. This binding scheme differs from that on the stoichiometric surface in two respects: the states of the stoichiometric surface at the bottom of the conduction band are empty and there are no 5c-Ti* sites on the surface.

E. Au_n fragmentation energies

We have calculated the energy of fragmentation of an adsorbed Au_n ($n=2-7$) cluster into adsorbed Au_{n-x} and adsorbed Au_x, by using the soft-oxygen pseudopotential and a $[5\times2]$ supercell. We put one fragment (Au_x) at its equilibrium position at the vacancy site (shown in the left column of Fig. 2) and the other one (Au_{n-x}) more than 6 Å away, at its equilibrium geometry on a stoichiometric region of the reduced surface. The geometry of the whole system is then optimized.

The dissociation energies of Au_n clusters ($n=2-7$), computed by using Eq. (2), are all positive (see the middle part in Table II), indicating that the fragmentation of Au_n is endothermic by at least 0.5 eV. The same thing was observed on the stoichiometric surface.[46] The kinetic energy of a fraction of mass-selected clusters deposited on a rutile TiO_2(110) single crystal exceeds 0.5 eV per cluster.[28,31,35,37,41,83] However scanning tunneling microscopy (STM) measurements do not observe cluster fragmentation upon impact.[28,31,83] A possible explanation is that they fragment and then recombine by the time when the STM image is taken. This is very unlikely: the mobility of the clusters on the surface is low and if they break and recombine they would not have all the same size (e.g., if Au_5 were to break into mobile Au_2 and a Au_3 clusters, one should observe Au_2, Au_3, Au_7, and Au_8 and this does not happen). The explanation for this is simple. The energy of the impact with the surface is spread over many degrees of freedom of the clusters and it takes time for it to pool, by accident, into the reaction coordinated leading to the breakup of the cluster. There is thus a competition between this energy pooling and the irreversible loss of energy by the cluster due to the interaction with the surface. The rate of the latter process is faster than the rate of the former, and this saves the cluster from breaking into pieces.

F. The interaction between coadsorbed clusters

The fragmentation energies calculated in the previous section include the interaction energy between the coadsorbed fragments. In the case of the stoichiometric surface, we have found that the presence of Au_3, or Au_5, or Au_7 on the surface increases substantially the binding energy of the monomer, even though the monomer was located at about 6 Å from the other cluster.[46] We examine here whether the reduced surface shows a similar phenomenon. To determine the interaction energy we calculate the fragmentation energy of the cluster so that the fragments do not interact with each other. We do this by using the following cycle. We start with Au_n in its lowest energy structure on the partially reduced rutile surface, desorb it into the gas phase, and relax its geometry to reach the lowest energy. The energy difference for this transition is the desorption energy of the intact cluster denoted $D_e[Au_n]$. Then we fragment Au_n into Au_{n-x} and Au_x in gas phase and optimize the structures of the fragments. The energy of this process is denoted $\delta_e[Au_n]_{gas}$ and its value is given in the upper part of Table II. Next, each fragment is adsorbed on a different TiO_2 slab: Au_x is adsorbed on a partially reduced surface, while Au_{n-x} is adsorbed on a stoichiometric surface. In other words, each fragment is *alone* in the unit cell of the slab. Moreover, the position of the fragments is the same as in the calculation of the fragmentation energy performed in the previous subsection, and their geometry is optimized. We denote the energies gained in this adsorption process by $D_e[Au_x]$ and $D_e[Au_{n-x}]$. The energy required to perform the cycle is

$$\delta_e[Au_n]_{cycle} = D_e[Au_n] + \delta_e[Au_n]_{gas} - D_e[Au_x] - D_e[Au_{n-x}]. \quad (4)$$

Obviously $\delta_e[Au_n]_{cycle}$ is the fragmentation energy in the hypothetical case when there is no interaction between the fragments. The difference between $\delta_e[Au_n]$, calculated, in the previous subsection, from Eq. (2) and the values of $\delta_e[Au_n]_{cycle}$ given by Eq. (4) is the interaction energy between the fragments. The results for $\delta_e[Au_n]$ and $\delta_e[Au_n]_{cycle}$ are given in the lower part of Table II. This table has a peculiar structure which is easiest to explain by giving and example. Let us look at the middle section which gives the

TABLE II. Dissociation energies (in eV) of small Au_n ($n=2-7$) clusters free and supported on a partially reduced rutile $TiO_2(110)$ surface. For example, Au_3 can dissociate into Au_1+Au_2, but only one fragment can occupy the vacancy site. The dissociation energies are 0.53 eV, when Au_1 is adsorbed at the vacancy site and Au_2 at its equilibrium structure on a stoichiometric patch, while it is 1.02 eV when Au_2 is sitting at the defect site and the monomer on the stoichiometric area located more that 6 Å from the defect site. The supported values were obtained with the combination of the PW91 functional and the soft-oxygen pseudopotential using a $[5\times2]$ supercell and a 12 layer thick slab.

	Fragment size (Au_x)[a]					
n	Au_1	Au_2	Au_3	Au_4	Au_5	Au_6
			$\delta_e[Au_n]$gas			
Au_2	2.28					
Au_3	1.30	1.30				
Au_4	2.53	1.56	2.53			
Au_5	2.21	2.47	2.47	2.21		
Au_6	3.04	2.97	4.20	2.97	3.04	
Au_7	1.60	2.36	3.27	3.27	2.36	1.60
			$\delta_e[Au_n]$[b]			
Au_2	0.50					
Au_3	0.53	1.02				
Au_4	0.63	0.91	0.85			
Au_5	0.60	1.16	0.90	0.97		
Au_6	0.77	1.34	1.34	1.27	1.16	
Au_7	0.81	1.50	1.51	1.79	1.49	1.21
			$\delta_e[Au_n]_{cycle}$[c]			
Au_2	0.46					
Au_3	0.55	0.99				
Au_4	0.65	0.91	0.83			
Au_5	0.63	1.17	0.90	0.98		
Au_6	0.78	1.34	1.34	1.24	1.17	
Au_7	0.84	1.51	1.53	1.71	1.45	1.19

[a]The fragment size indicated for the reduced surface corresponds to the one sitting at the location of a missing bridging oxygen, while the complementary part is sitting on a stoichiometric area of the surface.
[b]Dissociation energies obtained when both fragments are adsorbed on the same surface. See Eq. (2) for definition.
[c]Dissociation energies obtained by the following cycle: remove Au_n from the surface, break it up into Au_{n-x} and Au_x in the gas phase, and adsorb Au_x on a partially reduced surface and Au_{n-x} on a stoichiometric rutile $TiO_2(110)$ surface. See Eq. (4) for definition.

energy $\delta_e[Au_n]$. In the row for Au_4 the first column tells us that $\delta_e[Au_n]=0.63$ eV, if the Au_4 cluster breaks into a Au_1 cluster located at the vacancy site and a Au_3 cluster located on a stoichiometric patch of the surface. The next column tells us that $\delta_e[Au_n]=0.91$ eV, if the Au_4 cluster breaks into a Au_2 cluster located at the vacancy site and a Au_2 cluster located at on a stoichiometric patch on the surface. Finally, the third column gives $\delta_e[Au_n]=0.85$ eV if Au_4 breaks into a Au_3 cluster located on vacancy and a Au_1 cluster located on a stoichiometric patch. The third section gives the values of $\delta_e[Au_n]_{cycle}$ organized in the same manner. The first section gives $\delta_e[Au_n]_{gas}$ and the table is symmetric because there are no special binding sites for the clusters formed by fragmentation in the gas phase.

The calculations show that $\delta_e[Au_n]_{cycle}$ and $\delta_e[Au_n]$ differ by less than 0.08 eV which is smaller than the accuracy of our calculations. This tells us that the interaction energy between the fragments is negligible.

In Fig. 8(a) we see that the monomer (when no other cluster is on the surface) binds very strongly ($D_e[Au_1]=1.21$ eV) to a $5c$-Ti which is rather far from the vacancy. In the absence of the vacancy the binding energy is 0.45 eV.[46] This enhancement of the bond strength happens because the formation of the vacancy places electrons at the bottom of the conduction band, which facilitates binding of Au_1 to the $5c$-Ti atoms. The presence of the vacancy on the surface has the same effect as the presence of a Au_n (odd n) on a stoichiometric surface; both affect the monomer bond to the surface through the same mechanism. The desorption energies in the two cases are very close to each other.

Remarkably, placing a Au_n cluster at the vacancy site has practically no effect on the binding of Au_1 [see Figs. 8(a)–8(h). The binding energy and the charge of the Au_n located at the vacancy are practically the same in Fig. 8 as in left column of Fig. 2; coadsorption of the clusters has no effect on their binding energy or on the amount of charge they exchange with the surface. The effect of the vacancy on the adsorption and the charge of the monomer is not modified when a Au_n is adsorbed at the vacancy site.

V. SUMMARY AND CONCLUSIONS

The binding mechanism described in this paper is another example showing the importance of the frontier molecular orbitals of Au clusters in determining their reactivity. It is rather common to assume that the surprising chemical

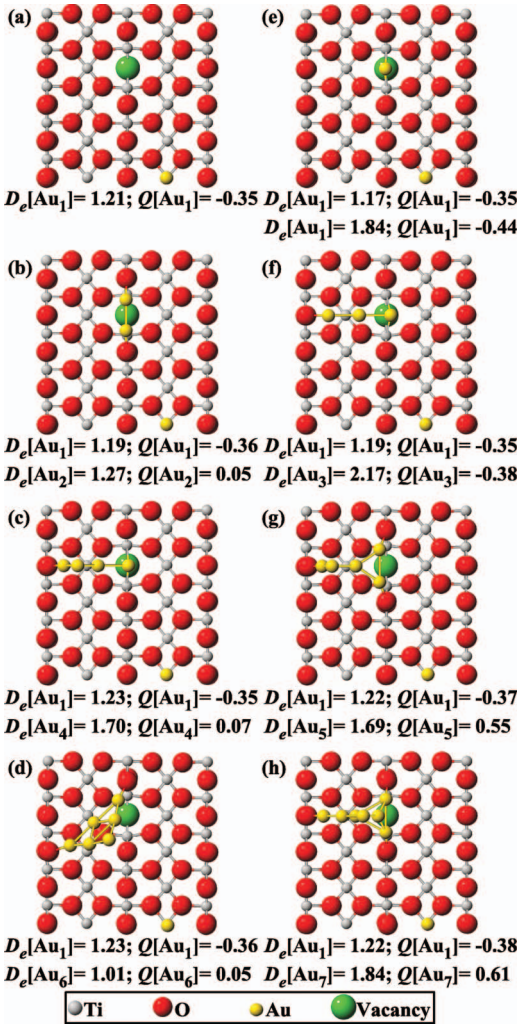

FIG. 8. (Color) Desorption (D_e) energies of Au monomer when a Au cluster, Au_n (n=0–7), is coadsorbed at a vacancy site on a partially reduced rutile TiO_2(110) surface. The results were obtained with the PW91 functional and the soft-oxygen pseudopotential on a [5×2] supercell and 12 layer slab. The energies are in eV. The total electronic charge on the Au clusters, Q, was obtained from Bader's charge analysis (Ref. 68).

activity of small Au cluster is due to the presence of low coordinated atoms on their surface. While this is true most of the time, the reality is more complicated. In our previous work[21,46,82,84–86] we have introduced the concept of "orbital roughness" and showed how it can be used to guess the bonding site of various molecules to gold clusters, by examining the frontier orbitals of the cluster without the adsorbate. Electron acceptors bind to the site on the bare cluster where the SOMO has a large lobe protruding into the vacuum. Electron donors bind to sites where the LUMO protrudes in the vacuum. It turns out that often the protruding lobes are located on the low coordination atoms. However, we have found examples in which the atom having the lowest coordination does not have a lobe of the frontier orbital protruding from it, and no molecule bind preferentially to that atom; the molecules bind to an atom having higher coordination and a large lobe of the frontier orbital.

The present calculations find that orbital roughness affects the manner in which gold clusters bind to the rutile surface. The most common bonding will maximize the overlap between the HOMOs of the free cluster and the eigenstate of the clean oxide localized on the bridging and the in-plane oxygens. The frontier MOs of the free Au clusters [see Figs. 4(e)–4(g), 5(b)–5(d), 6(e), 6(f), 7(c), and 7(d)] have lobes at the edge of the clusters and not on the flat side of the cluster. This is the main reason why Au_n clusters interact with protruding bridging oxygen atoms located on each side of the missing bridging oxygen [see Figs. 2(b) and 2(e)–2(g)] and the defect site [see Figs. 2(c) and 2(d)] through Au atoms located at the edges of the cluster. This binding mode maximized the orbital overlap and the number of Au–O bonds. Low-lying isomers were obtained for Au_3 [see Fig. 2(c)] and Au_4 (not shown) in which an "inside" atom is sitting over the defect but they are 0.1 eV (Au_3) and 0.3 eV (Au_4) higher in energy than the structures presented in Fig. 2.

Maximization of the orbital overlap between the HOMOs of the free cluster and the eigenstate of the clean oxide localized on oxygens atoms can be invoked to explain the structural changes observed upon adsorption. For instance, Au_5 and Au_7 are both planar (2D) in the gas phase,[60–62,87] while they both adopt a 3D shape upon adsorption [see Figs. 2(e) and 2(g)]. The importance of oxygen atoms in the binding is further supported by the fact that Au_n (n=2–7) clusters are adsorbed between two adjacent protruding bridging oxygen rows on the partially reduced (see Figs. 2 and 3) and stoichiometric rutile TiO_2(110) surfaces.[46] This is in agreement with scanning tunneling microscopy imaging following deposition of mass-selected Au clusters on TiO_2(110) −(1×1) showing that most of the signal attributed to Au clusters is centered between bridging oxygen rows.[31,83]

The importance of orbital roughness is further illustrated by the observation that the participation of the 5c-Ti atoms in the binding between Au_n clusters and the support is determined by the shape and the orientation of LUMO for even n and SOMO for odd n. Among all the possible structures formed by various ligations of the same Au cluster, only those in which the LUMO (or SOMO for odd n) has a large lobe pointing in the direction of a 5c-Ti atom in the surface layer (located or not at the vacancy site) lead to the formation of a bonding MO between the LUMO of Au_n and the eigenstates of the clean oxide located at the bottom of the conduction band (see Figs. 4 and 5). This binding state is located in the band gap allowing the electronic density to flow in from the conduction band. This results in an accumulation of a negative charge on the cluster. Otherwise, the 5c-Ti atoms do not participate in the binding and Au_n clusters with even n stay neutral, while those with odd n donate electrons into the conduction band becoming positively charged.

The effect of the vacancy is local: the bond strength of the clusters located away from the vacancy is close to the one calculated for the stoichiometric surface (see Fig. 3). The only exception is Au_1: the presence of the vacancy allows Au_1 to bind strongly to the 5c-Ti atoms far from the vacancy site. This behavior has been explained by the binding mechanism presented above.

Upon binding on a stoichiometric area of the partially reduced surface, a cluster changes its shape and orientation

to maximize the orbital overlap between its frontier MOs and the eigenstates of the clean oxide involving bridging and in-plane oxygen atoms. By doing so, the LUMO for even n and the SOMO for odd n do not point in the direction of a $5c$-Ti atom. This excludes the participation of the $5c$-Ti atom in the binding and prevent charging of the cluster from the support. Therefore, in a mass-selected cluster experiment there will be two kinds of clusters: those that bind at the vacancy site and those that bind away from it. Those at the vacancy site form stronger bonds with the surface and some of them could be negatively charged. The ones away from vacancies are more weakly bound and will be either charged positively or not at all.

Au_1 behavior is different from that of larger cluster in many respects. Its binding strength is greatly enhanced on the partially reduced surface compared to the stoichiometric one and the presence of oxygen vacancies increases its adsorption energy on all the $5c$-Ti atoms regardless how far they are from a vacancy site. Once again, this can be explained by the binding mechanism presented here. Upon Au monomer adsorption on the rutile $TiO_2(110)$ surface, a partially filled MO is formed by the overlap of the SOMO of Au_1 and eigenstates of the clean oxide located in the conduction band. This binding state is located in the band gap allowing electronic density to flow in from the conduction band. The conduction band is empty for the stoichiometric surface, preventing electron transfer from the support. This is why Au_1 binding to the stoichiometric surface is only 0.45 eV and its charge is $+0.05e$. In contrast, the creation of oxygen vacancies partially populates the conduction band allowing electronic density to flow into the binding state involving the SOMO of the monomer. This enhances the monomer binding to 1.81 eV at the vacancy site and to $\sim$1.2 eV on the $5c$-Ti atoms. The effect of the vacancy is very delocalized in the case of the monomer because the eigenstates involved in the creation of a bonding MO with the SOMO have amplitude over all the $5c$-Ti atoms [see Fig. 1(b)].

ACKNOWLEDGMENTS

This work was supported by the Air Force Office of Scientific Research under Grant No. FAA9550-06-1-0167 and under a Defense University Research Initiative on Nanotechnology (DURINT) Grant No. F49620-01-1-0459. We are grateful to the Hewlett-Packard and to the California Nano-Systems Institute (CNSI) for computer resources obtained from a NSF grant (CHE-0321368). We want to thank Greg Mills, Lauren Benz, Xiao Tong, and Steve K. Buratto for helpful discussions.

[1] E. Wahlström, N. Lopez, R. Schaub, P. Thostrup, A. Rønnau, C. Africh, E. Lægsgaard, J. K. Nørskov, and F. Besenbacher, Phys. Rev. Lett. **90**, 026101 (2003).
[2] X. Tong, L. Benz, A. Kolmakov, S. Chrétien, H. Metiu, and S. K. Buratto, Surf. Sci. **575**, 60 (2005).
[3] A. Vijay, G. Mills, and H. Metiu, J. Chem. Phys. **118**, 6536 (2003).
[4] Y. Wang and G. S. Hwang, Surf. Sci. **542**, 72 (2003).
[5] J. A. Rodriguez, G. Liu, T. Jirsak, J. Hrbek, Z. P. Chang, J. Dvorak, and A. Maiti, J. Am. Chem. Soc. **124**, 5242 (2002).
[6] N. Lopez and J. K. Nørskov, Surf. Sci. **515**, 175 (2002).
[7] Z. Yang, R. Wu, Q. Zhang, and D. W. Goodman, Phys. Rev. B **65**, 155407 (2002).
[8] A. Vittadini and A. Selloni, J. Chem. Phys. **117**, 353 (2002).
[9] A. Sanchez, S. Abbet, U. Heiz, W.-D. Schneider, H. Häkkinen, R. N. Barnett, and U. Landman, J. Phys. Chem. A **103**, 9573 (1999).
[10] H. Häkkinen, S. Abbet, A. Sanchez, U. Heiz, and U. Landman, Angew. Chem., Int. Ed. Engl. **42**, 1297 (2003).
[11] B. Yoon, H. Häkkinen, U. Landman, A. S. Wörz, J.-M. Antonietti, S. Abbet, K. Judai, and U. Heiz, Science **307**, 403 (2005).
[12] Z. Yan, S. Chinta, A. A. Mohamed, J. P. Fackler, Jr., and D. W. Goodman, J. Am. Chem. Soc. **127**, 1604 (2005).
[13] T. H. Lee and K. M. Ervin, J. Phys. Chem. **98**, 10023 (1994).
[14] B. E. Salisbury, W. T. Wallace, and R. L. Whetten, Chem. Phys. **262**, 131 (2000).
[15] W. T. Wallace and R. L. Whetten, J. Am. Chem. Soc. **124**, 7499 (2002).
[16] W. T. Wallace, A. J. Leavitt, and R. L. Whetten, Chem. Phys. Lett. **368**, 774 (2003).
[17] J. Hagen, L. D. Socaciu, W. Elijazyfer, U. Heiz, T. M. Bernhardt, and L. Wöste, Phys. Chem. Chem. Phys. **4**, 1707 (2002).
[18] Y. D. Kim, M. Fischer, and G. Ganteför, Chem. Phys. Lett. **377**, 170 (2003).
[19] D. Stolcic, M. Fischer, G. Ganteför, Y. D. Kim, Q. Sun, and P. Jena, J. Am. Chem. Soc. **125**, 2848 (2003).
[20] G. Mills, M. S. Gordon, and H. Metiu, Chem. Phys. Lett. **359**, 493 (2002).
[21] G. Mills, M. S. Gordon, and H. Metiu, J. Chem. Phys. **118**, 4198 (2003).
[22] B. Yoon, H. Häkkinen, and U. Landman, J. Phys. Chem. A **107**, 4066 (2003).
[23] X. Ding, Z. Li, J. Yang, J. G. Hou, and Q. Zhu, J. Chem. Phys. **120**, 9594 (2004).
[24] M. L. Kimble, A. W. Castleman, Jr., R. Mitrić, C. Bürgel, and V. Bonačić-Koutecký, J. Am. Chem. Soc. **126**, 2526 (2004).
[25] A. Franceschetti, S. J. Pennycook, and S. T. Pantelides, Chem. Phys. Lett. **374**, 471 (2003).
[26] W. T. Wallace, R. B. Wyrwas, R. L. Whetten, R. Mitrić, and V. Bonačić-Koutecký, J. Am. Chem. Soc. **125**, 8408 (2003).
[27] L. M. Molina and B. Hammer, J. Chem. Phys. **123**, 161104 (2005).
[28] P. Kemper, A. Kolmakov, X. Tong, Y. Lilach, L. Benz, M. Manard, H. Metiu, S. K. Buratto, and M. T. Bowers, Int. J. Mass. Spectrom. **254**, 202 (2006).
[29] L. Benz, X. Tong, P. Kemper, H. Metiu, M. T. Bowers, and S. K. Buratto, J. Phys. Chem. B **110**, 663 (2006).
[30] X. Tong, L. Benz, S. Chrétien, P. Kemper, A. Kolmakov, H. Metiu, M. T. Bowers, and S. K. Buratto, J. Chem. Phys. **123**, 204701 (2005).
[31] X. Tong, L. Benz, P. Kemper, H. Metiu, M. T. Bowers, and S. K. Buratto, J. Am. Chem. Soc. **127**, 13516 (2005).
[32] L. Benz, X. Tong, P. Kemper, Y. Lilach, A. Kolmakov, H. Metiu, M. T. Bowers, and S. K. Buratto, J. Chem. Phys. **122**, 081102 (2005).
[33] M. Arenz, U. Landman, and U. Heiz, ChemPhysChem **7**, 1871 (2006).
[34] A. S. Wörz, U. Heiz, F. Cinquini, and G. Pacchioni, J. Phys. Chem. B **109**, 18418 (2005).
[35] S. Lee, C. Fan, T. Wu, and S. L. Anderson, J. Chem. Phys. **123**, 124710 (2005).
[36] S. Lee, C. Fan, T. Wu, and S. L. Anderson, J. Phys. Chem. B **109**, 11340 (2005).
[37] S. Lee, C. Fan, T. Wu, and S. L. Anderson, Surf. Sci. **578**, 5 (2005).
[38] K. Judai, A. S. Wörz, S. Abbet, J.-M. Antonietti, U. Heiz, A. Del Vitto, L. Giordano, and G. Pacchioni, Phys. Chem. Chem. Phys. **7**, 955 (2005).
[39] A. Del Vitto, L. Giordano, G. Pacchioni, and U. Heiz, J. Phys. Chem. B **109**, 3416 (2003).
[40] A. S. Wörz, K. Judai, S. Abbet, J.-M. Antonietti, U. Heiz, A. Del Vitto, L. Giordano, and G. Pacchioni, Chem. Phys. Lett. **399**, 266 (2004).
[41] S. Lee, C. Fan, T. Wu, and S. L. Anderson, J. Am. Chem. Soc. **126**, 5682 (2004).
[42] M. Aizawa, S. Lee, and S. L. Anderson, Surf. Sci. **542**, 253 (2003).
[43] K. Judai, S. Abbet, A. S. Wörz, U. Heiz, L. Giordano, and G. Pacchioni, J. Phys. Chem. B **107**, 9377 (2003).
[44] K. Judai, S. Abbet, A. S. Wörz, A. M. Ferrari, L. Giordano, G. Pacchioni, and U. Heiz, J. Mol. Catal. A: Chem. **199**, 103 (2003).
[45] U. Diebold, Surf. Sci. Rep. **48**, 53 (2003).
[46] S. Chrétien and H. Metiu, J. Chem. Phys. **127**, 084704 (2007).
[47] G. Kresse and J. Hafner, Phys. Rev. B **47**, 558 (1993).
[48] G. Kresse and J. Hafner, Phys. Rev. B **49**, 14251 (1994).
[49] G. Kresse and J. Furthmüller, Comput. Mater. Sci. **6**, 15 (1996).
[50] G. Kresse and J. Furthmüller, Phys. Rev. B **54**, 11169 (1996).

[51] J. P. Perdew, J. A. Chevary, S. H. Vosko, K. A. Jackson, M. R. Pederson, D. J. Singh, and C. Fiolhais, Phys. Rev. B **46**, 6671 (1992).
[52] J. P. Perdew, J. A. Chevary, S. H. Vosko, K. A. Jackson, M. R. Pederson, D. J. Singh, and C. Fiolhais, Phys. Rev. B **48**, 4978E (1993).
[53] J. P. Perdew, K. Burke, and Y. Wang, Phys. Rev. B **54**, 16533 (1996).
[54] J. P. Perdew, K. Burke, and Y. Wang, Phys. Rev. B **57**, 14999E (1998).
[55] D. Vanderbilt, Phys. Rev. B **41**, 7892 (1990).
[56] D. Pillay and G. S. Hwang, Phys. Rev. B **72**, 205422 (2005).
[57] G. Makov and M. C. Payne, Phys. Rev. B **51**, 4014 (1995).
[58] P. Pulay, Chem. Phys. Lett. **73**, 393 (1980).
[59] W. H. Press, S. A. Teukolsky, W. T. Vetterling, and B. P. Flannery, *Numerical Recipes in Fortran: The Art of Scientific Computing* (Cambridge University Press, Cambridge, 1992).
[60] L. Xiao and L. Wang, Chem. Phys. Lett. **392**, 452 (2004).
[61] J. Wang, G. Wang, and J. Zhao, Phys. Rev. B **66**, 035418 (2002).
[62] H. Häkkinen and U. Landman, Phys. Rev. B **62**, R2287 (2000).
[63] L. Xiao, B. Tollberg, X. Hu, and L. Wang, J. Chem. Phys. **124**, 114309 (2006).
[64] H. Häkkinen, B. Yoon, U. Landman, X. Li, H.-J. Zhai, and L.-S. Wang, J. Phys. Chem. A **107**, 6168 (2003).
[65] F. Furche, R. Ahlrichs, P. Weis, C. Jacob, S. Gilb, T. Bierweiler, and M. M. Kappes, J. Chem. Phys. **117**, 6982 (2002).
[66] S. Gilb, P. Weis, F. Furche, R. Ahlrichs, and M. M. Kappes, J. Chem. Phys. **116**, 4094 (2002).
[67] R. F. W. Bader, *Atoms in Molecules—A Quantum Theory* (Oxford University Press, Oxford, 1990).
[68] G. Henkelman, A. Arnaldsson, and H. Jónsson, Comput. Mater. Sci. **36**, 354 (2006).
[69] E. Sanville, S. D. Kenny, R. Smith, and G. Henkelman, J. Comput. Chem. **28**, 899 (2007).
[70] M. V. Ganduglia-Pirovano, A. Hofmann, and J. Sauer, Surf. Sci. Rep. **62**, 219 (2007).
[71] C. Di Valentin, G. Pacchioni, and A. Selloni, Phys. Rev. Lett. **97**, 166803 (2006).
[72] A. D. Becke, J. Chem. Phys. **98**, 5648 (1993).
[73] P. J. Stephens, F. J. Devlin, C. F. Chabalowski, and M. J. Frisch, J. Phys. Chem. **98**, 11623 (1994).
[74] X. Wu, A. Selloni, and S. K. Nayak, J. Chem. Phys. **120**, 4512 (2004).
[75] D. Pillay and G. S. Hwang, J. Mol. Struct. **771**, 129 (2006).
[76] J. G. Wang and B. Hammer, Phys. Rev. Lett. **97**, 136107 (2006).
[77] D. Matthey, J. G. Wang, S. Wendt, J. Matthiesen, R. Schaub, E. Lægsgaard, B. Hammer, and F. Besenbacher, Science **315**, 1692 (2007).
[78] K. J. Taylor, C. L. Pettiette-Hall, O. Cheshnovsky, and R. E. Smalley, J. Chem. Phys. **96**, 3319 (1992).
[79] J. Ho, K. M. Ervin, and W. C. Lineberger, J. Chem. Phys. **93**, 6987 (1990).
[80] P. E. Blöchl, Phys. Rev. B **50**, 17953 (1994).
[81] G. Kresse and D. Joubert, Phys. Rev. B **59**, 1758 (1999).
[82] S. Chrétien and H. Metiu, J. Chem. Phys. **126**, 104701 (2007).
[83] S. K. Buratto, M. T. Bowers, H. Metiu, M. Manard, X. Tong, L. Benz, P. Kemper, and S. Chrétien, in *The Chemical Physics of Solid Surfaces*, Atomic Clusters From Gas Phase to Deposited Vol. 12, edited by D. P. Woodruff (Elsevier, Amsterdam, 2006), Chap. 4, pp. 151–199.
[84] S. Chrétien, M. S. Gordon, and H. Metiu, J. Chem. Phys. **121**, 3756 (2004).
[85] S. Chrétien, M. S. Gordon, and H. Metiu, J. Chem. Phys. **121**, 9925 (2004).
[86] S. Chrétien, M. S. Gordon, and H. Metiu, J. Chem. Phys. **121**, 9931 (2004),.
[87] W. Fa, C. Luo, and J. Dong, Phys. Rev. B **72**, 205428 (2005).